Radiation Measurements 142 (2021) 106558

Contents lists available at ScienceDirect

Radiation Measurements

journal homepage: http://www.elsevier.com/locate/radmeas

Optimized method for individual radon progeny measurement based on alpha spectrometry following the Wicke method

Yunxiang Wang [a], Changhao Sun [b,c], Lei Zhang [b,*], Qiuju Guo [a]

[a] State Key Laboratory of Nuclear Physics and Technology, School of Physics, Peking University, Beijing, 100871, China
[b] State Key Laboratory of NBC Protection for Civilian, Beijing, 102205, China
[c] School of Nuclear Science and Technology, University of South China, Hengyang, Hunan, 421001, China

ARTICLE INFO

Keywords:
Radon progeny
Alpha spectrometry
Activity concentration
The wicke method
Comparison measurement

ABSTRACT

Accurate measurement of individual short-lived radon progeny concentrations is very important for dose evaluation and related researches taking radon progeny as radioactive tracers. Different methods have been developed, but higher methodological sensitivity is needed for field measurement under the limitation of size, weight and power consumption of the instrument. For the purpose of developing new measurement method with higher sensitivity, an optimized method based on alpha spectrometry following the Wicke method (Wicke, 1979) is demonstrated, which shortens the measurement cycle to 60 min and make it more suitable for field measurement. For comparison, a series of verification experiments were carried out, and the methodological sensitivity and uncertainty were analyzed in detail in this paper. Results show that the optimized Wicke method can give accurate individual radon progeny concentrations and equilibrium equivalent concentration (EEC) in different environments. The deviation between EEC measured by the optimized Wicke method and the original Wicke method is less than ±2.9%, and the deviation between the optimized Wicke method and the Kerr method is less than ±3.9% in different environment. The methodological sensitivity of the optimized Wicke method is nearly the same as the original method with a much shorter measurement cycle, and 4.3 times higher than that of the Kerr method, which lowers the measurement uncertainty especially in the actual environment.

1. Introduction

Radon and its progeny are not only the greatest contributor of the natural radiation background to human exposure (UNSCEAR, 2000), but also important radioactive tracers for environmental, geophysical as well as atmospheric studies (Baskaran, 2016). For radon exposure dose assessment through dosimetry approach, serval characteristic parameters of radon progeny are required, and the ratio of activity concentrations of individual short-lived radon progeny ^{218}Po, ^{214}Pb and ^{214}Bi is one of them (ICRP, 2017). So accurate measurement on individual radon progeny not only leads to equilibrium equivalent concentration (EEC) or potential alpha energy concentration (PAEC), but also can provide basic parameters for dose evaluation. On the other hand, taking individual radon progeny as effective tracers for atmospheric study, continuous measurement on radon progeny is a necessary tool, and 1-h measurement cycle is usually demanded with the parallel to other meteorological factors (Crova et al., 2021).

Compared with the direct measurement of EEC or PAEC, the measurement of individual radon progeny is more difficult and requires higher sensitivity (NCRP, 1988). For this purpose, numerous measurement methods have been developed in the past few decades, including both alpha-counting methods (Tsivoglou et al., 1953; Thomas, 1970, 1972; Cliff, 1978a/1978b; Busigin and Phillips, 1980; Scott, 1981; Nazaroff, 1984), alpha-spectrometry methods (Martz et al., 1969; Jonassen and Hayes, 1974; Kerr, 1975; Hill, 1975; Nazaroff et al., 1981; Nazaroff, 1983) and alpha-beta spectrometry methods (Rolle and Lettner, 1996; Katona et al., 2007). Most of them use three alpha count periods or three alpha-beta count periods to analytical solve the activity concentrations of ^{218}Po, ^{214}Pb and ^{214}Bi.

With the increasing demand for accurate field survey, radon progeny monitor has been continuously improved in sensitivity and lower limit of detection. Due to the limitation of size, weight and power consumption of portable instruments, it is very important to achieve higher sensitivity of radon progeny measurement by the optimization of measurement procedure, with the same sampling flowrate and detection efficiency. In the past, the Kerr method (Kerr, 1975) based on 0–10 min

* Corresponding author.
E-mail address: swofely@pku.edu.cn (L. Zhang).

https://doi.org/10.1016/j.radmeas.2021.106558
Received 4 November 2020; Received in revised form 19 February 2021; Accepted 5 March 2021
Available online 11 March 2021

sampling process and two alpha spectrum measurement intervals of 12–22 min and 25–40 min, was pointed out by Kadir (Kadir et al., 2013) to be more efficient than other methods based on alpha counts and analytical solutions, and it is used in a step-advanced filter radon progeny monitors (Zhang et al., 2017) and also used as a reference in the national radon chamber at National Institute of Metrology (NIM) of China (Liang et al., 2015). However, a method with higher methodological sensitivity still needs to be developed for field measurement. Longer sampling and optimized counting time can bring higher sensitivity and lower uncertainty. To achieve the purpose, Duggan and Howell (1968) formerly developed a method which simultaneously records alpha spectrum while sampling for 30 min, and measures the second spectrum after 30 min' waiting. After that, Wicke (1979) realized the method with cycle of 90 min, which samples and measures for the first 30 min at the same time, and measures for another 30 min after 30 min' waiting. Due to its longer sampling and measuring time, the Wicke method has a much higher sensitivity than the Kerr method. However, measurement cycle of 90 min is not quite suitable for continuous field measurement. The 1-h cycle has unparalleled advantage in continuous measurement for long-term observation, not only in the field of radiological protection but also in related studies that taking radon progeny as tracers. Taking atmospheric study as an example, 1-h cycle measurement of radon progeny can be synchronous with other common meteorological monitoring, which is expected for better analysis.

For the purpose of developing a new measurement method with higher sensitivity and 1-h cycle, an optimized method following the original Wicke method was demonstrated in this paper, and a series of comparison experiments among the optimized Wicke method, the original Wicke method and the Kerr method were carried out in different environments, and the methodological sensitivity and measurement uncertainty were also analyzed in this paper.

2. Materials and methods

2.1. Measurement methods

The sampling time of the original Wicke method is synchronized with the first measurement interval of 0–30 min, then there is a 30-min waiting time and the second measurement interval is 60–90 min. Relatively long sampling time and measurement while sampling, make the original Wicke method to have a higher sensitivity than other alpha spectrometry method or alpha-counting method, but its 90-min cycle is not suitable for field measurement and hourly monitoring. In order to achieve hourly measurement of radon progeny, some modification to the original Wicke method is needed. Considering the great advantage of sampling and measuring at the same time, the optimized Wicke method retains the same sampling time and first measurement interval of 0–30 min, but shortens the waiting time from 30 min to 10 min in order to shorten the total cycle to 1 h. So the second measurement interval was adjusted to 40–60 min, just as shown in Fig. 1. For comparison, the sampling and measuring processes of the Kerr method are also shown in Fig. 1.

All the three methods have one sampling interval and two measurement intervals, and typical alpha spectra of two measurement intervals are shown in Fig. 2. The half-life of ^{218}Po is only 3.09 min, while the half-lives of ^{214}Pb and ^{214}Bi are 26.8 and 19.9 min, respectively. This difference makes alpha particles from ^{218}Po (6.00 MeV) only appear in the first measurement interval. And due to relatively longer half-lives of ^{214}Pb and ^{214}Bi, alpha particles from ^{214}Po (7.69 MeV) can be seen in both two intervals. Using this property, reasonably arranging two measurement intervals, the relationship between ^{218}Po, ^{214}Pb and ^{214}Bi concentrations and alpha counts of different regions of interest (ROI) in two spectra can be established.

The following assumptions are made for simplicity. (1) Concentrations of ^{218}Po, ^{214}Pb and ^{214}Bi remain constant during the sampling process; (2) The filter has the same collection efficiency for ^{218}Po, ^{214}Pb and ^{214}Bi; (3) Ignore the difference between the detection efficiency for 6.0 MeV and 7.69 MeV alpha particles; (4) The flowrate remains stable and constant during the sampling process.

Take N_1, N_2 and N_3 as alpha counts of ROI-I in the first interval, ROI-II in the first interval, and ROI-II in the second interval, separately. Using Bateman equations (Bateman, 1910) and recurrence formulas discussed by Jenkins (2002), the relationship between individual radon progeny concentrations C_1, C_2, C_3, and N_1, N_2, N_3 are shown in Eq. (1) and Eq. (2).

$$\begin{pmatrix} C_1 \\ C_2 \\ C_3 \end{pmatrix} = \varepsilon_\alpha^{-1} \cdot F^{-1} \cdot \varepsilon_f^{-1} \cdot \begin{pmatrix} M_{11} & M_{12} & M_{13} \\ M_{21} & M_{22} & M_{23} \\ M_{31} & M_{32} & M_{33} \end{pmatrix} \begin{pmatrix} N_1 \\ N_2 \\ N_3 \end{pmatrix} \tag{1}$$

$$\sigma_{Ci} = C_i \cdot \sqrt{\frac{(M_{i1})^2 \cdot N_1 + (M_{i2})^2 \cdot N_2 + (M_{i3})^2 \cdot N_3}{(M_{i1} \cdot N_1 + M_{i2} \cdot N_2 + M_{i3} \cdot N_3)^2} + \left(\frac{\sigma_{\varepsilon\alpha}}{\varepsilon_\alpha}\right)^2 + \left(\frac{\sigma_{\varepsilon f}}{\varepsilon_f}\right)^2 + \left(\frac{\sigma_F}{F}\right)^2} \tag{2}$$

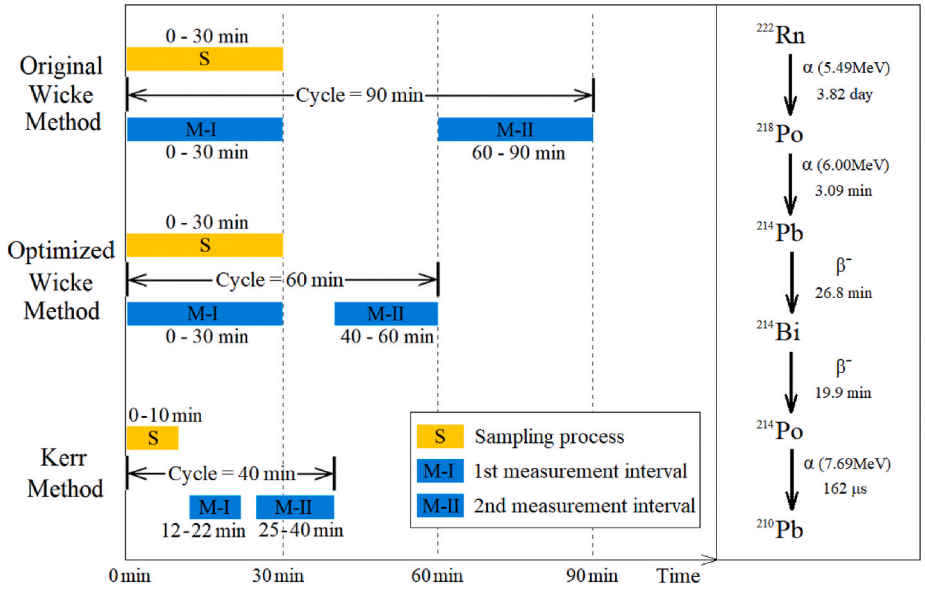

Fig. 1. Schematic diagram of sampling process and measurement intervals of three methods (left), and the decay scheme of radon (right).

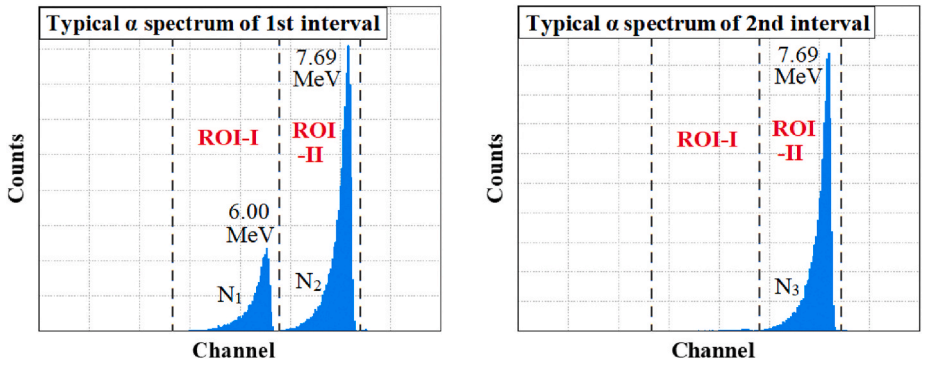

Fig. 2. Typical alpha spectra of two measurement intervals with ROI-I (5.0–6.2 MeV) and ROI-II (6.2–7.8 MeV) for the optimized Wicke method.

Where C_1, C_2, C_3 are the activity concentrations of ^{218}Po, ^{214}Pb and ^{214}Bi (Bq/m^3). ε_α is the alpha detection efficiency, F is the sampling flowrate (L/min), ε_f is the collection efficiency of the filter, and corresponding uncertainties are $\sigma_{\varepsilon\alpha}$, σ_F and $\sigma_{\varepsilon f}$. $\widehat{M}$ is the matrix related to specific measurement methods (see the Appendix for the detailed derivation). For the optimized Wicke method, the sampling process and the first measurement interval are both from 0 to 30 min, and the second measurement interval is from 40 to 60 min, so the corresponding matrix $\widehat{M}$ should be as following Eq. (3).

$$\widehat{M}_{\text{Optimized Wicke}} = \begin{pmatrix} 0.14709 & 0 & 0 \\ -0.018402 & -0.022921 & 0.062012 \\ 0.0021013 & 0.058218 & -0.019385 \end{pmatrix} \quad (3)$$

EEC and its uncertainty (Bq/m^3) can be obtained from Eq. (4) and Eq. (5) as follow.

$$EEC = 0.105 \cdot C_1 + 0.516 \cdot C_2 + 0.379 \cdot C_3 \quad (4)$$

$$\sigma_{\text{EEC}} = \sqrt{0.011 \cdot \sigma_{C1}{}^2 + 0.266 \cdot \sigma_{C2}{}^2 + 0.144 \cdot \sigma_{C3}{}^2} \quad (5)$$

2.2. Comparison experiments

For the verification, comparison experiments were carried out separately in the radon chamber at NIM, in a basement, and in an office room from November to December in 2019. Three step-advanced filter radon progeny monitors RPM-SF01 (Sairatec, China) (Zhang et al., 2017) were used in the comparison experiment, which were made-in-order and corresponding measurement procedures and calculation programs of the three methods were written into the instruments. The sampling flowrate was calibrated to be 2.50 ± 0.10 L/min, which is traced to national standard by Gilian Gilibrator-2 Calibrator (Sensidyne, USA). The alpha detection efficiencies of three instruments were calibrated to be (22.9 ± 1.1)%, (20.7 ± 1.0)% and (21.3 ± 1.1)% using electroplated ^{241}Am source, and the collection efficiency of the 0.45 μm PTFE filter (Haichengshijie, China) is 100% (SD: 3%).

For comparison, the aerosol concentration was adjusted in the radon chamber in order to cover a wide range of EEC and C(^{218}Po):C(^{214}Pb):C(^{214}Bi). In the basement and the office room, air purifiers were used for a change in the aerosol concentration.

The radon chamber at NIM has a total volume of nearly 20 m^3 including an exposure volume of 12.44 m^3 with devices to stably control radon concentration and aerosol concentration (Liang et al., 2015). The comparison experiment in the radon chamber lasted for 48 h. In the first 24 h, radon concentration in the chamber was set to 2500 Bq/m^3 with aerosol concentration of 1000 particles/cm^3. Then in the second 24 h, radon concentration was set to 5000 Bq/m^3 with aerosol concentration of 10000 particles/cm^3.

The basement for comparison experiment has a size of 5 m × 3 m × 3 m with an AC5655 air purifier (Phillips, Netherlands). The experiment in the basement lasted for 100 h and radon concentration was measured by an RTM 2200 radon monitor (SARAD, Germany). In the first 55 h, the air purifier was turned off. After 55 h, the air purifier was turned on and switched to minimum speed to reduce the aerosol concentration. The door of the basement was closed during the experiment but opened once at about 30th hour to check the status of the instruments.

The office room has a size of 5 m × 4.4 m × 3.2 m with door and windows closed, and a 270E Slim air purifier (Blueair, Sweden) was placed in. The experiment in the office room lasted for 100 h. In the first 50 h, the air purifier was off. After 50 h, the air purifier was turned on. Radon concentration in the room was continuously measured by a RAD7 radon monitor (Durridge, USA).

3. Results and discussion

3.1. Comparison results in three different environments

Comparison results of three measurement methods in the radon chamber, basement and office room are shown in Fig. 3. EEC and ^{218}Po, ^{214}Pb and ^{214}Bi concentrations given by the optimized Wicke method, the original Wicke method and the Kerr method are separately listed in each figure with different marks and colors. Radon concentrations in different environments are also shown in the figures along with EEC as a reference.

In the radon chamber at NIM (Fig. 3(a)), average radon concentration increased from 2650 Bq/m^3 to 5180 Bq/m^3 with EEC accordingly increasing from 705 Bq/m^3 to 3120 Bq/m^3, and ^{218}Po, ^{214}Pb, ^{214}Bi concentrations are also increased after adjusting the aerosol concentration. In the basement (Fig. 3(b)), average radon concentration changed from 1710 Bq/m^3 to 1760 Bq/m^3, and average EEC decreased significantly from 680 Bq/m^3 to 52 Bq/m^3 before and after the air purifier was turned on. ^{218}Po, ^{214}Pb, ^{214}Bi concentrations also went down significantly. It is worth noting that the ^{218}Po concentration increased stably after the air purifier was on, mainly due to the increase of radon concentration. In the office room (Fig. 3(c)), average radon concentration changed from 199 Bq/m^3 to 102 Bq/m^3 before and after the air purifier was on, while average EEC dropped significantly from 85 Bq/m^3 to 3.6 Bq/m^3, and ^{218}Po, ^{214}Pb, ^{214}Bi concentrations had similar trends. The phenomenon that air purifiers significantly decreased the proportion of ^{214}Pb and ^{214}Bi both in the basement and office room, was also observed in former researches (Wang et al., 2011; Iwaoka et al., 2013).

By changing aerosol concentration, different radon progeny environments had been realized with different EECs and activity concentration ratios. The average results of three methods in each experiment phases are listed in Table 1, in which phase 1 and phase 2 stand for before and after aerosol adjustment in the radon chamber, phase 3/4 stands for air purifier off/on in the basement, and phase 5/6 is for air purifier off/on in the office room. The average EEC ranges from 3.5 Bq/m^3 to 3120 Bq/m^3, spanning three orders of magnitude, and individual radon progeny concentrations are also with a large variety due to

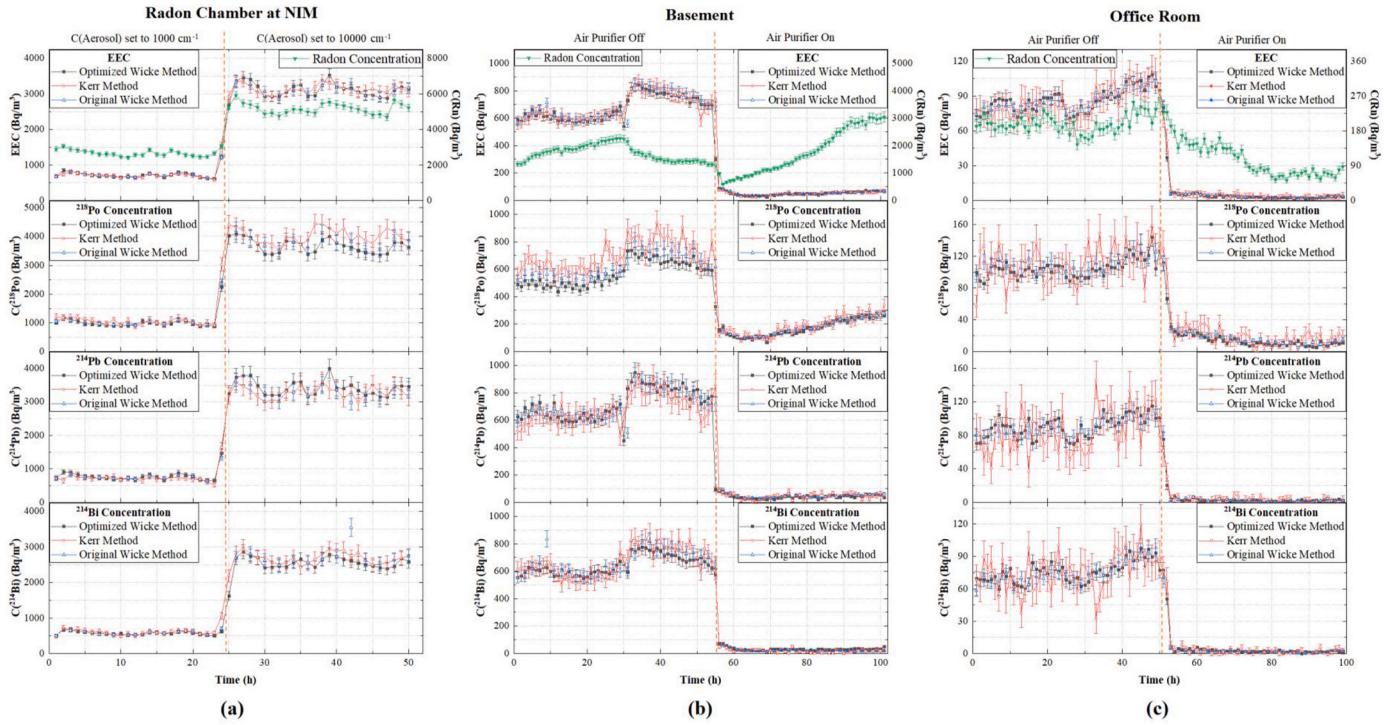

Fig. 3. Comparison results of three measurement methods in radon chamber, basement and office room.

Table 1
Average radon progeny concentrations of the three measurement methods in different experimental phases.

Measurement Method	Measurement Sites	Radon Chamber at NIM		Basement		Office Room	
	Experiment Phases	Phase 1	Phase 2	Phase 3	Phase 4	Phase 5	Phase 6
	Rn Concentration (Bq/m^3)	2650 ± 170	5180 ± 300	1710 ± 300	1760 ± 820	199 ± 25	102 ± 39
Optimized Wicke Method	EEC (Bq/m^3)	709 ± 34	3110 ± 150	671 ± 34	53 ± 4	86 ± 6	3.5 ± 0.8
	C(^{218}Po) (Bq/m^3)	979 ± 71	3680 ± 360	569 ± 42	171 ± 14	105 ± 9	13 ± 2
	C(^{214}Pb) (Bq/m^3)	758 ± 57	3420 ± 250	712 ± 54	43 ± 6	90 ± 10	2.3 ± 1.2
	C(^{214}Bi) (Bq/m^3)	571 ± 42	2540 ± 180	645 ± 48	33 ± 4	76 ± 7	2.4 ± 0.8
Original Wicke Method	EEC (Bq/m^3)	704 ± 33	3120 ± 140	688 ± 33	52 ± 3	86 ± 5	3.4 ± 0.6
	C(^{218}Po) (Bq/m^3)	998 ± 72	3800 ± 270	628 ± 46	176 ± 14	110 ± 10	16 ± 2
	C(^{214}Pb) (Bq/m^3)	745 ± 54	3280 ± 230	715 ± 52	49 ± 5	89 ± 8	2.2 ± 0.9
	C(^{214}Bi) (Bq/m^3)	569 ± 42	2710 ± 190	699 ± 49	23 ± 3	75 ± 7	1.8 ± 0.6
Kerr Method	EEC (Bq/m^3)	701 ± 46	3120 ± 160	680 ± 46	51 ± 9	84 ± 12	3.8 ± 2.2
	C(^{218}Po) (Bq/m^3)	1050 ± 90	4020 ± 310	695 ± 68	183 ± 27	112 ± 20	18 ± 7
	C(^{214}Pb) (Bq/m^3)	712 ± 75	3280 ± 260	687 ± 74	47 ± 14	85 ± 20	2.3 ± 2.2
	C(^{214}Bi) (Bq/m^3)	593 ± 58	2670 ± 210	669 ± 62	21 ± 9	75 ± 15	1.8 ± 1.6

different aerosol and radon concentration. The lowest concentrations appeared in the office room when the air purifier was on, and the highest appeared in the radon chamber with 5000 Bq/m^3 radon concentration and 10000 particles/cm^3 aerosol concentration.

In such a variety of radon progeny concentration, comparison results show that all the three methods can quickly respond to the change of individual radon progeny concentrations consistently in all the three environments, and the difference between three measurement methods are within the uncertainty of EEC and ^{218}Po, ^{214}Pb, ^{214}Bi concentrations. For the measurement of EEC, the results given by the two Wicke methods are less than ±2.9% in all the six phases. For the results of ^{218}Po, ^{214}Pb and ^{214}Bi, the deviations of the two Wicke methods are basically less than ±9.4%, ±4.4% and ±6.3%, respectively. Comparing the optimized Wicke method with the Kerr method, the difference of EEC is less than ±3.9% at different concentration levels except for the lowest concentration in phase 6, and the deviations of ^{214}Pb and ^{214}Bi concentrations are basically less than ±6.5% and ±4.9%. But for ^{218}Po concentration, the results given by the Kerr method are a little higher than the two Wicke methods at all the six phases with an average value of 18%, which needs further analysis, but its variety is quite larger than those of the two Wicke methods, especially in the basement and in the office room. Higher ^{218}Po concentration of the Kerr method make its avarage C(^{214}Pb):C(^{218}Po) and C(^{214}Bi):C(^{218}Po) ratios in phase 3 are smaller than one, while the C(^{214}Pb):C(^{218}Po) and C(^{214}Bi):C(^{218}Po) ratios given by the two Wicke methods in phase 3 are larger than one. This phenomenon that C(^{214}Pb) and C(^{214}Bi) are greater than C(^{218}Po) seems not physically correct. The possible reason is that the recoil energy produced in the decay process of deposited ^{218}Po, will make part of ^{214}Pb return to the air, which leads to higher concentration of ^{214}Pb and ^{214}Bi.

3.2. Sensitivity and uncertainty analysis

Different sampling and measuring processes will give different counts under the same sampling flowrate, detection efficiency and radon progeny concentration. Methodologically, sensitivity refers to the counting rate measured at unit radon progeny concentration, under normalized flowrate and detection efficiency. The higher is the

sensitivity of a method, the smaller is the counting statistical uncertainty.

For comparison, Table 2 lists the average normalized counting numbers of three methods in three EEC levels. Results show that normalized counting numbers under unit flowrate and detection efficiency $N_i/\varepsilon_\alpha/F$ increase with radon progeny concentration. Comparing the normalized N_1 of the optimized Wicke method in ^{218}Po measurement, it is 10.5 times higher than the Kerr method, which is mainly due to triple synchronized sampling and measurement time than the Kerr method. Normalized N_2 and N_3 counts of the optimized Wicke method are also 4.3 and 3.7 times higher than those of the Kerr method. So the overall sensitivity of the optimized Wicke method is at least 4.3 times higher than that of the Kerr method.

For the two Wicke methods, the optimized Wicke method shortens the second measurement interval from 60-90 min to 40–60 min, but also shortens the waiting time from 30 min to 10 min, so its normalized counting numbers are comparable with original method and the difference is only less than 4.3%, which has little effect on total sensitivity.

The lower limit of detection (LLD) depends partly on the performance of instruments and partly on the sensitivity of the method used. According to the theory of ISO 11929 (2019), the LLDs of the three methods can be calculated by Eq. (6), using the instrumental background, collection and detection efficiency, sampling flowrate, and the methodological sensitivity based on the specific measurement procedure.

$$LLD = \frac{M\cdot\left(2.71 + 4.65\cdot\sqrt{BG}\right)}{\varepsilon_\alpha\cdot\varepsilon_f\cdot F} \tag{6}$$

In Eq. (6), M is the sensitivity coefficient related to the matrix $\widehat{M}$ in Eq. (1), and BG is the background counts during the measurement. The background counting rates of RPM-SF01 radon progeny monitors used in this study are 3.6 cph in ROI-I and 2.7 cph in ROI-II (Zhang et al., 2017). The measurement of ^{218}Po is only related to N_1, so the LLD for ^{218}Po is easy to calculate. However, the calculation of ^{214}Pb, ^{214}Bi and EEC involves the real-time ratio of radon progeny, so only the equilibrium LLD is given for comparison. For the optimized Wicke method, LLDs for ^{218}Po, ^{214}Pb, ^{214}Bi and EEC measurement are 2.5 Bq/m^3, 0.20 Bq/m^3, 0.15 Bq/m^3 and 0.39 Bq/m^3, respectively. For the original Wicke method, the LLDs are 2.3 Bq/m^3, 0.19 Bq/m^3, 0.14 Bq/m^3 and 0.36 Bq/m^3. For the Kerr method, four LLDs are 20 Bq/m^3, 0.61 Bq/m^3, 0.45 Bq/m^3 and 1.2 Bq/m^3. Obviously, the LLDs of two Wicke methods are much better than those of the Kerr method. Little difference between two Wicke methods mainly caused by different detection efficiency of two instruments.

The optimized Wicke method promotes the methodological sensitivity and lowers the uncertainty. But for one measurement system, measurement uncertainty is composed of not only counting statistical uncertainty related to sensitivity, but also the inherent systematic uncertainty related to calibration issues, just as shown in Eq. (2). For comparison, Table 3 lists the counting statistical uncertainty e_{stats_Po}, e_{stats_Pb}, e_{stats_Bi} and inherent systematic uncertainty e_{sys} of RPM-SF01 monitors at three EEC levels. The systematic uncertainty e_{sys} is the inherent quality of the measurement system, which is related to calibration issues such as flowrate, detection efficiency and collection efficiency, and is expressed as $e_{sys}^2 = \left(\frac{\sigma_{e\alpha}}{\varepsilon_\alpha}\right)^2 + \left(\frac{\sigma_{ef}}{\varepsilon_f}\right)^2 + \left(\frac{\sigma_F}{F}\right)^2$.

The comparison results show that the statistical uncertainty goes down with the growing EEC, while the systematic uncertainty remains constant for all the three methods. Increasing the sensitivity of a method can minimize the contribution of counting statistical uncertainty to the overall uncertainty. At EEC level of 3120 Bq/m^3, the inherent systematic uncertainty is the main source of overall uncertainty for all the three methods. At EEC level of 705 Bq/m^3, the statistical uncertainty of the two Wicke methods is still the main contribution to total uncertainty. But for the Kerr method, its statistical uncertainty has increased to a level comparable to the systematic uncertainty. At EEC level of 85 Bq/m^3, fewer counts further increase the statistical uncertainties of the Wicke methods to be comparable to systematic uncertainty, while for the Kerr method, the statistical uncertainty increases significantly to be the main contribution to overall uncertainty. The optimized Wicke method has much smaller counting statistical uncertainty than the Kerr method, making it more suitable for field measurement.

Actually, for different arrangements of sampling and measuring processes with 1-h cycle, the methodological uncertainty was also theoretically analyzed. The result shows that the optimized Wicke method has relatively low uncertainty, and it is significant especially at low concentration levels. Since the experimental comparison results have proved that the optimized Wicke method can meet the demands of high sensitivity and 1-h cycle, the result of theoretical uncertainty analysis will not be discussed in this paper.

4. Conclusions

For hourly measurement of radon progeny concentration with high sensitivity, an optimized Wicke method was developed from the original Wicke method, and comparison experiments were carried out in three different environments. Results show that the optimized Wicke method can give accurate individual radon progeny concentrations and EEC in different environments. The deviation between EEC measured by the optimized Wicke method and the original Wicke method is less than ±2.9%, and the deviation between the optimized Wicke method and the Kerr method is less than ±3.9%. The methodological sensitivity of the optimized Wicke method is nearly the same as the original method, and at least 4.3 times higher than that of the Kerr method.

The optimized Wicke method retains the advantage of high methodological sensitivity of the original Wicke method, while meets the needs of hourly measurement of individual radon progeny

Table 2
Average normalized counting numbers given by the three methods at three EEC levels.

Measurement Methods	EEC Levels	3120 Bq/m^3	705 Bq/m^3	85 Bq/m^3
Optimized Wicke Method	$N_1/\varepsilon_\alpha/F$	24900	6700	720
	$N_2/\varepsilon_\alpha/F$	73300	16300	2090
	$N_3/\varepsilon_\alpha/F$	85100	19100	2350
	Total	**183300**	**42100**	**5160**
Original Wicke Method	$N_1/\varepsilon_\alpha/F$	25700	6759	750
	$N_2/\varepsilon_\alpha/F$	74800	16128	2060
	$N_3/\varepsilon_\alpha/F$	88000	19935	2410
	Total	**188500**	**42822**	**5220**
Kerr Method	$N_1/\varepsilon_\alpha/F$	2400	620	70
	$N_2/\varepsilon_\alpha/F$	16800	3710	460
	$N_3/\varepsilon_\alpha/F$	23100	5110	620
	Total	**42300**	**9440**	**1150**

Table 3
Compositions of uncertainties given by the three methods at three EEC levels.

Measurement Methods	EEC Levels	3120 Bq/m^3	705 Bq/m^3	85 Bq/m^3
Optimized Wicke Method	e_{stats_Po}	0.9%	1.7%	5.2%
	e_{stats_Pb}	1.2%	2.6%	7.7%
	e_{stats_Bi}	1.1%	2.3%	6.2%
	e_{sys}	7.1%	7.1%	7.1%
Original Wicke Method	e_{stats_Po}	0.8%	1.6%	5.0%
	e_{stats_Pb}	0.8%	1.7%	5.0%
	e_{stats_Bi}	0.8%	1.9%	5.1%
	e_{sys}	7.1%	7.1%	7.1%
Kerr Method	e_{stats_Po}	2.8%	5.5%	16.9%
	e_{stats_Pb}	3.6%	7.8%	22.8%
	e_{stats_Bi}	3.1%	6.7%	18.5%
	e_{sys}	7.1%	7.1%	7.1%

concentration. At EEC of 85 Bq/m^3, the uncertainty of EEC measurement by the two Wicke methods mainly comes from the systematic uncertainty, while for the Kerr method it mainly comes from the statistical uncertainty.

Actually, radon progeny concentration in most environment is not so high, especially in indoor environment and atmosphere. Higher methodological sensitivity usually means lower uncertainty and higher accuracy, under the limited conditions such as size, weight, noise and power consumption, which is very important for field survey and continuous measurement. So the optimization of sampling and detecting processes, and the promotion of methodological sensitivity will be quite important. It is believed that the requirement of accurate measurement on individual radon progeny in indoor environments will increase when taking dosimetric modeling approach for dose evaluation from exposure to radon progeny as suggested in ICRP Publication 115 (2010). And in the future, the interference of thoron (^{220}Rn) will also be considered.

Declaration of competing interest

The authors declare that they have no known competing financial interests or personal relationships that could have appeared to influence the work reported in this paper.

Acknowledgements

This study is financially supported by National Natural Science Foundation of China (No.11775009).

Appendix

To use the recurrence formulas, the following h factors and f factors need to be defined.

$$\begin{cases} h_{11} = (1 - e^{-\lambda_1 t_s})/\lambda_1 \\ h_{22} = (1 - e^{-\lambda_2 t_s})/\lambda_2 \\ h_{33} = (1 - e^{-\lambda_3 t_s})/\lambda_3 \\ h_{12} = (h_{11} - h_{22})/(\lambda_2 - \lambda_1) \\ h_{23} = (h_{22} - h_{33})/(\lambda_3 - \lambda_2) \\ h_{13} = (h_{12} - h_{23})/(\lambda_3 - \lambda_1) \end{cases} \tag{A.1}$$

$$\begin{cases} f_{11} = e^{-\lambda_1 t_d} \\ f_{22} = e^{-\lambda_2 t_d} \\ f_{33} = e^{-\lambda_3 t_d} \\ f_{12} = (f_{11} - f_{22})/(\lambda_2 - \lambda_1) \\ f_{23} = (f_{22} - f_{33})/(\lambda_3 - \lambda_2) \\ f_{13} = (f_{12} - f_{23})/(\lambda_3 - \lambda_1) \end{cases} \tag{A.2}$$

Where t_s and t_d are time variables in sampling and decay processes, and λ_1, λ_2, λ_3 are the decay constants of ^{218}Po, ^{214}Pb, ^{214}Bi, respectively. h factors are used in the sampling process and f factors are used in the decay process after sampling.

For a specific sampling process, assume that the concentrations of ^{218}Po, ^{214}Pb, ^{214}Bi in the air are C_1, C_2, C_3, the sampling flowrate is F, and the collection efficiency of the filter is ε_f. Take the beginning of sampling as zero for t_s, the individual radon progeny activities on the filter A_1, A_2, A_3 at any time during sampling process can be described as following equations with h factors.

$$\begin{cases} A_1(t_s) = F \cdot \varepsilon_f \cdot h_{11} \cdot C_1 \\ A_2(t_s) = F \cdot \varepsilon_f \cdot (\lambda_2 \cdot h_{12} \cdot C_1 + h_{22} \cdot C_2) \\ A_3(t_s) = F \cdot \varepsilon_f \cdot (\lambda_2 \cdot \lambda_3 \cdot h_{13} \cdot C_1 + \lambda_3 \cdot h_{23} \cdot C_2 + h_{33} \cdot C_3) \end{cases} \tag{A.3}$$

After the sampling process, there is no more collection of radon progeny. Take the end of sampling as zero for t_d, the radon progeny activities on the filter at any time during decay process can be as following equations with f factors.

$$\begin{cases} A_1(t_d) = A_{1se} \cdot f_{11} = F \cdot \varepsilon_f \cdot h_{11se} \cdot f_{11} \cdot C_1 \\ A_2(t_d) = \lambda_2 \cdot A_{1se} \cdot f_{12} + A_{2se} \cdot f_{22} \\ = F \cdot \varepsilon_f \cdot [\lambda_2 \cdot (h_{11se} \cdot f_{12} + h_{12se} \cdot f_{22}) \cdot C_1 + h_{22se} \cdot f_{22} \cdot C_2] \\ A_3(t_d) = \lambda_2 \cdot \lambda_3 \cdot A_{1se} \cdot f_{13} + \lambda_3 \cdot A_{2se} \cdot f_{23} + A_{3se} \cdot f_{33} \\ = F \cdot \varepsilon_f \cdot \begin{bmatrix} \lambda_2 \cdot \lambda_3 \cdot (h_{11se} \cdot f_{13} + h_{12se} \cdot f_{23} + h_{13se} \cdot f_{33}) \cdot C_1 \\ + \lambda_3 \cdot (h_{22se} \cdot f_{23} + h_{23se} \cdot f_{33}) \cdot C_2 + h_{33se} \cdot f_{33} \cdot C_3 \end{bmatrix} \end{cases} \tag{A.4}$$

Where A_{1se}, A_{2se}, A_{3se} are the individual radon progeny activities on the filter, and h_{ijse} are h factors at the end of sampling process t_{se}, which can be derived by substituting $t_s = t_{se}$ into Eq.(A.1) and Eq.(A.3).

For any specific measurement interval from $t_1$to,t_2 if the measurement efficiency for alpha particles is,ε_α counts of ROI-I and ROI-II can be integrated as follows.

$$\begin{cases} N_{218} = \varepsilon_\alpha \cdot \int_{t_1}^{t_2} A_1(t) dt \\ N_{214} = \varepsilon_\alpha \cdot \int_{t_1}^{t_2} A_3(t) dt \end{cases} \tag{A.5}$$

If the measurement interval is in the sampling process, $A_i(t_s)$ in Eq.(A.3) should be integrated in Eq.(A.5). Otherwise, if the measurement interval is in the decay process after sampling, i$A_i(t_d)$n Eq.(A.4) should be substituted into Eq.(A.5).

As shown in Fig. 2, for two-interval measurement, ROI-I counts of first interval, ROI-II counts of first interval, and ROI-II counts of second interval

are usually used as N_1, N_2 and N_3 to analytical solve radon progeny concentrations C_1, C_2 and C_3. If interval A ($t_{A1}\sim t_{A2}$) is in sampling process and interval B ($t_{B1}\sim t_{B2}$) is during decay process (like the Wicke methods), the relationship between radon progeny concentrations and ROI counts is expressed by following Eq.(A.6).

$$\begin{cases} N_1 = \varepsilon_\alpha \cdot F \cdot \varepsilon_f \cdot \int_{t_{A1}}^{t_{A2}} h_{11} dt_s \cdot C_1 \\ N_2 = \varepsilon_\alpha \cdot F \cdot \varepsilon_f \cdot \left[\lambda_2 \cdot \lambda_3 \cdot \int_{t_{A1}}^{t_{A2}} h_{13} \mathrm{d}t_s \cdot C_1 + \lambda_3 \cdot \int_{t_{A1}}^{t_{A2}} h_{23} \mathrm{d}t_s \cdot C_2 + \int_{t_{A1}}^{t_{A2}} h_{33} \mathrm{d}t_s \cdot C_3 \right] \\ N_3 = \varepsilon_\alpha \cdot F \cdot \varepsilon_f \cdot \left[\begin{array}{l} \lambda_2 \cdot \lambda_3 \cdot \left(h_{11se} \cdot \int_{t_{B1}}^{t_{B2}} f_{13} \mathrm{d}t_d + h_{12se} \cdot \int_{t_{B1}}^{t_{B2}} f_{23} \mathrm{d}t_d + h_{13se} \cdot \int_{t_{B1}}^{t_{B2}} f_{33} \mathrm{d}t_d \right) \cdot C_1 \\ + \lambda_3 \cdot \left(h_{22se} \cdot \int_{t_{B1}}^{t_{B2}} f_{23} \mathrm{d}t_d + h_{23se} \cdot \int_{t_{B1}}^{t_{B2}} f_{33} \mathrm{d}t_d \right) \cdot C_2 + h_{33se} \cdot \int_{t_{B1}}^{t_{B2}} f_{33} dt_d \cdot C_3 \end{array} \right] \end{cases} \tag{A.6}$$

If interval A and interval B are both in decay process after sampling (such as the Kerr method), the relationship can be described as Eq.(A.7).

$$\begin{cases} N_1 = \varepsilon_\alpha \cdot F \cdot \varepsilon_f \cdot h_{11se} \cdot \int_{t_{A1}}^{t_{A2}} f_{11} dt_d \cdot C_1 \\ N_2 = \varepsilon_\alpha \cdot F \cdot \varepsilon_f \cdot \left[\begin{array}{l} \lambda_2 \cdot \lambda_3 \cdot \left(h_{11se} \cdot \int_{t_{A1}}^{t_{A2}} f_{13} \mathrm{d}t_d + h_{12se} \cdot \int_{t_{A1}}^{t_{A2}} f_{23} \mathrm{d}t_d + h_{13se} \cdot \int_{t_{A1}}^{t_{A2}} f_{33} \mathrm{d}t_d \right) \cdot C_1 \\ + \lambda_3 \cdot \left(h_{22se} \cdot \int_{t_{A1}}^{t_{A2}} f_{23} \mathrm{d}t_d + h_{23se} \cdot \int_{t_{A1}}^{t_{A2}} f_{33} \mathrm{d}t_d \right) \cdot C_2 + h_{33se} \cdot \int_{t_{A1}}^{t_{A2}} f_{33} dt_d \cdot C_3 \end{array} \right] \\ N_3 = \varepsilon_\alpha \cdot F \cdot \varepsilon_f \cdot \left[\begin{array}{l} \lambda_2 \cdot \lambda_3 \cdot \left(h_{11se} \cdot \int_{t_{B1}}^{t_{B2}} f_{13} \mathrm{d}t_d + h_{12se} \cdot \int_{t_{B1}}^{t_{B2}} f_{23} \mathrm{d}t_d + h_{13se} \cdot \int_{t_{B1}}^{t_{B2}} f_{33} \mathrm{d}t_d \right) \cdot C_1 \\ + \lambda_3 \cdot \left(h_{22se} \cdot \int_{t_{B1}}^{t_{B2}} f_{23} \mathrm{d}t_d + h_{23se} \cdot \int_{t_{B1}}^{t_{B2}} f_{33} \mathrm{d}t_d \right) \cdot C_2 + h_{33se} \cdot \int_{t_{B1}}^{t_{B2}} f_{33} dt_d \cdot C_3 \end{array} \right] \end{cases} \tag{A.7}$$

So far, the linear relationship between 218Po, 214 Pb, 214Bi concentrations C_1, C_2, $C_3$and counts of interested regions,N_1 ,N_2 hN_3as been established, which can simply be expressed in matrix form as follow.

$$\begin{pmatrix} N_1 \\ N_2 \\ N_3 \end{pmatrix} = \varepsilon_\alpha \cdot F \cdot \varepsilon_f \cdot \begin{pmatrix} K_{11} & K_{12} & K_{13} \\ K_{21} & K_{22} & K_{23} \\ K_{31} & K_{32} & K_{33} \end{pmatrix} \begin{pmatrix} C_1 \\ C_2 \\ C_3 \end{pmatrix} \tag{A.8}$$

Where matrix elements K_{ij} are the corresponding linear coefficients in Eq.(A.6) and Eq.(A.7). Inverse Eq.(A.8) and we have Eq.(A.9) and Eq.(A.10).

$$\begin{pmatrix} C_1 \\ C_2 \\ C_3 \end{pmatrix} = \varepsilon_\alpha^{-1} \cdot F^{-1} \cdot \varepsilon_f^{-1} \cdot \begin{pmatrix} M_{11} & M_{12} & M_{13} \\ M_{21} & M_{22} & M_{23} \\ M_{31} & M_{32} & M_{33} \end{pmatrix} \begin{pmatrix} N_1 \\ N_2 \\ N_3 \end{pmatrix} \tag{A.9}$$

$$\widehat{\boldsymbol{M}} = \begin{pmatrix} M_{11} & M_{12} & M_{13} \\ M_{21} & M_{22} & M_{23} \\ M_{31} & M_{32} & M_{33} \end{pmatrix} = \widehat{\boldsymbol{K}}^{-1} = \begin{pmatrix} K_{11} & K_{12} & K_{13} \\ K_{21} & K_{22} & K_{23} \\ K_{31} & K_{32} & K_{33} \end{pmatrix}^{-1} \tag{A.10}$$

In this paper, the specific forms of matrix $\widehat{\boldsymbol{M}}$ for the three methods are derived by substituting specific sampling time and measurement intervals. For the optimized Wicke method, the sampling process and the first measurement interval are both from 0 to 30 min, and the second measurement interval is from 40 to 60 min. For the original Wicke method, the sampling process and the first measurement interval are both from 0 to 30 min, and the second measurement interval is from 60 to 90 min. For the Kerr method, the sampling process is from 0 to 10 min, and the first measurement interval is from 12 to 22 min, and the second measurement interval is from 25 to 40 min. So the corresponding matrixes of these three methods are shown as Eq.(A.11–13) respectively. The units of radon progeny concentrations and flowrate should be Bq/m^3 and L/min in the calculation.

$$\widehat{\boldsymbol{M}}_{\text{Optimized Wicke}} = \begin{pmatrix} 0.1471 & 0 & 0 \\ -0.01775 & -0.05213 & 0.09043 \\ 0.001897 & 0.06735 & -0.02827 \end{pmatrix} \tag{A.11}$$

$$\widehat{\boldsymbol{M}}_{\text{Original Wicke}} = \begin{pmatrix} 0.1471 & 0 & 0 \\ -0.01840 & -0.02292 & 0.06201 \\ 0.002101 & 0.05822 & -0.01939 \end{pmatrix} \tag{A.12}$$

$$\widehat{\boldsymbol{M}}_{\text{Kerr}} = \begin{pmatrix} 1.686 & 0 & 0 \\ -0.2078 & -0.3939 & 0.4502 \\ 0.03003 & 0.4197 & -0.1921 \end{pmatrix} \tag{A.13}$$

References

Baskaran, M., 2016. In: Radon: a Tracer for Geological, Geophysical and Geochemical Studies. Springer International Publishing, Switzerland. https://doi.org/10.1007/978-3-319-21329-3.

Bateman, H., 1910. The solution of a system of differential equations of radioactive decay. Proc. Camb. Phil. Soc. 15, 423–427.

Busigin, A., Phillips, C.R., 1980. Uncertainties in the measurement of airborne radon daughters. Health Phys. 39, 943–955. https://doi.org/10.1097/00004032-198012000-00008.

Cliff, D.K., 1978a. The measurement of low concentrations of radon-222 daughters in air, with emphasis on RaA assessment. Phys. Med. Biol. 23, 55–65. https://doi.org/10.1088/0031-9155/23/1/005.

Cliff, D.K., 1978b. Revised coefficients for the measurement of radon-222 daughter concentrations in air. Phys. Med. Biol. 23, 1206–1209. https://doi.org/10.1088/0031-9155/23/6/423.

Durridge Co Inc, 2021. RAD7 radon detector. Last time accessed on 2021-2-1. https://durridge.com/products/rad7-radon-detector.

Crova, F., Valli, G., Bernardoni, V., Forello, A.C., Valentini, S., Vecchi, R., 2021. Effectiveness of airborne radon progeny assessment for atmospheric studies. Atmos. Res. 250, 105390. https://doi.org/10.1016/j.atmosres.2020.105390.

Duggan, M.J., Howell, D.M., 1968. A method for measuring the concentrations of the short-lived daughter products of radon-222 in the atmosphere. Int. J. Appl. Radiat. Isot. 19, 865–870. https://doi.org/10.1016/0020-708x(68)90165-8.

Haichengshijie Filter Equipment Co Ltd, 2021. PTFE filter. Last time accessed on. http://www.hcsjgl.com/show.asp?id=65.

Hill, A., 1975. Rapid measurement of radon, decay products, unattached fractions, and working level values of mine atmospheres. Health Phys. 28, 472–474. PMID: 1120683.

International Commission on Radiological Protection ICRP, 2017. ICRP Publication 137. In: Occupational Intakes of Radionuclides, vol. 3. ISBN: 9781526440167.

International Commission on Radiological Protection ICRP, 2010. ICRP Publication 115: Lung Cancer Risk from Radon and Progeny and Statement on Radon, ISBN 978-0-7020-4977-4.

International Standard Organization (ISO), 2019. ISO 11929: Determination of the Characteristic Limits (Decision Threshold, Detection Limit and Limits of the Confidence Interval) for Measurements of Ionizing Radiation-Fundamentals and Application.

Iwaoka, K., Tokonami, S., Ishikawa, T., Yonehara, H., 2013. Mitigation effects of radon decay products by air cleaner. J. Radioanal. Nucl. Chem. 295, 639–642. https://doi.org/10.1007/s10967-012-1813-z.

Jenkins, P.H., 2002. Equations for modeling of grab samples of radon decay products. Health Phys. 83, S48–S51. https://doi.org/10.1097/00004032-200208001-00014.

Jonassen, N., Hayes, E.I., 1974. A correction when measuring ^{222}Rn daughter concentrations by alpha spectroscopy of filter samples. Health Phys. 27, 310–313. PMID: 4436055.

Kadir, A., Zhang, L., Guo, Q., Liang, J., 2013. Efficiency analysis and comparison of different radon progeny measurement methods. Sci. World J. 269168. https://doi.org/10.1155/2013/269168, 2013.

Katona, T., Kanyar, B., Somlai, J., Molnar, A., 2007. Determining ^{222}Rn daughter activities by simultaneous alpha- and beta-counting and modeling. J. Radioanal. Nucl. Chem. 272, 69–74. https://doi.org/10.1007/s10967-006-6793-4.

Kerr, G.D., 1975. Measurement of Radon Progeny Concentrations in Air by Alpha-Particle Spectrometry. Oak Ridge National Laboratory Report. ORNL-TM-4924.

Liang, J., Zheng, P., Yang, Z., Liu, H., Zhang, M., Li, Z., Zhang, L., Guo, Q., 2015. Development of calibration facility for radon and its progenies at NIM (China). Radiat. Protect. Dosim. 167, 82–86. https://doi.org/10.1093/rpd/ncv222.

Martz, D.E., Holleman, D.F., McCurdy, D.E., Schiager, K.J., 1969. Analysis of atmospheric concentrations of RaA, RaB and RaC by alpha spectroscopy. Health Phys. 17, 131–138. https://doi.org/10.1097/00004032-196907000-00014.

National Council on Radiation Protection and Measurements NCRP, 1988. NCRP Report No. 97: Measurement of Radon and Radon Daughters in Air, ISBN 0-913392-97-9.

Nazaroff, W.W., 1983. Radon daughter carousel: an automated instrument for measuring indoor concentrations of ^{218}Po, ^{214}Pb, and ^{214}Bi. Rev. Sci. Instrum. 54, 1227–1233. https://doi.org/10.1063/1.1137555.

Nazaroff, W.W., 1984. Optimizing the total-alpha three-count technique for measuring concentrations of radon progeny in residences. Health Phys. 46, 395–405. https://doi.org/10.1097/00004032-198402000-00015.

Nazaroff, W.W., Nero, A.V., Revzan, K.L., 1981. Alpha Spectroscopic Techniques for Field Measurements of Radon Daughters. Second Special Symposium on Natural Radiation Environment, Bombay, India. https://escholarship.org/uc/item/2wh7z3fn.

Phillips (China) Investment Co. Ltd.. AC5655 air purifier. Last time accessed on 2021-2-1. https://www.philips.com.cn/c-p/AC5655_00/series-5000i-air-purifier.

Rolle, R., Lettner, H., 1996. An analysis of efficient measurement procedures for radon progeny. Environ. Int. 22, S585–S593. https://doi.org/10.1016/S0160-4120(96)00159-6.

Sairatec Co Ltd, 2021. RPM-SF01 radon progeny monitor. Last time accessed on 2021-2-1. http://www.sairatec.com/teamview_5999939.html.

SARAD GmbH. RTM 2200 radon and thoron measurement system. Last time accessed on 2021-2-1. https://www.sarad.de/product-detail.php?lang=en_US&cat_ID=1&p_ID=25.

Scott, A.G., 1981. A field method for measurement of radon daughters in air. Health Phys. 41, 403–405. PMID: 7275629.

Sensidyne, L.P.. Gilian Gilibrator-2 NIOSH primary standard air flow calibrator. Last time accessed on 2021-2-1. https://www.sensidyne.com/air-sampling-equipment/calibration-equipment/gilibrator-2/.

Blueair Shanghai Sales Co. Ltd.. Classic 270E Slim air purifier. Last time accessed on 2021-2-1. https://www2.blueair.com/cn/air-purifiers/classic-270e-slim.

Thomas, J.W., 1970. Modification of the Tsivoglou method for radon daughters in air. Health Phys. 19, 691. PMID: 5513685.

Thomas, J.W., 1972. Measurement of radon daughters in air. Health Phys. 23, 783–789. https://doi.org/10.1097/00004032-197212000-00004.

Tsivoglou, E.C., Ayer, H.E., Holaday, D.A., 1953. Occurrence of nonequilibrium atmospheric mixtures of radon and its daughters. Nucleonics 11 (40). OSTI: 4410365.

United Nations Scientific Committee on the Effects of Atomic Radiation (UNSCEAR), 2000. Sources and Effects of Ionizing Radiation, vol. I. United Nations Publications, 92-1-142238-8.

Wang, J., Meisenberg, O., Chen, Y., Karg, E., Tschiersch, J., 2011. Mitigation of radon and thoron decay products by filtration. Sci. Total Environ. 409, 3613–3619. https://doi.org/10.1016/j.scitotenv.2011.06.030.

Wicke, A., 1979. Untersuchungen zur Frage der Naturlichen Radioactivitat der Luft in Wohn und Aufenthaltsraumen. Ph.D. thesis. University of Giessen.

Zhang, L., Yang, J., Guo, Q., 2017. Study on a step-advanced filter monitor for continuous radon progeny measurement. Radiat. Protect. Dosim. 173, 259–262. https://doi.org/10.1093/rpd/ncw333.